Exact solution of the electrostatic problem for a single-electron dual-junction-array trap

2000 J. Phys.: Condens. Matter 12 4641

(http://iopscience.iop.org/0953-8984/12/21/308)

J. Phys.: Condens. Matter **12** (2000) 4641–4653. Printed in the UK PII: S0953-8984(00)11018-5

Exact solution of the electrostatic problem for a single-electron dual-junction-array trap

Jai Yon Ryu†‡, Sang Chil Lee†‡, G Y Hu‡ and C S Ting‡

† Department of Physics, Cheju National University, Cheju 690–756, Korea

‡ Texas Center for Superconductivity, University of Houston, TX 77204, USA

Received 14 January 2000

Abstract. We present an exact analytical solution to the electrostatic problem of the biased single-electron dual-junction-array trap, which consists of equal stray capacitances C_0, equal junction capacitances C, equal input gate capacitances C_1, and a coupling capacitance C_C. The threshold voltages are investigated for various charge solitons including a single electron, an exciton, and a combined exciton and single electron. Our results show that their threshold voltages have strong dependences on the cotunnelling, C_0/C, C_1/C, C_C/C, and the number of junctions, and that various types of charge soliton transport occur according to these parameters. Previous discussions in the literature have neglected the effect of the stray capacitance, but we find that the effect plays an important role in the charge soliton transport.

1. Introduction

Since Likharev's report [1] on single-electron tunnelling (SET) devices whose fundamental operation principle is based on the Coulomb blockade effect, a lot of work has been carried out [2–12] on the physics of SET phenomena and on the wide variety of SET device applications. One of the most significant SET systems is the single-electron 'trap', which is comprised of a junction array and a capacitor as shown in figure 1(a). It serves as a memory cell by holding an electron or a hole in the trap, i.e., a '0' state for no extra charge in the trap and a '1' state for an extra charge in the trap. Numerous papers have already been published [5–9, 12] on this subject. Recently, Amakawa, Fujishima, and Hoh [10] presented a more complicated single-electron memory circuit, a single-electron dual-junction-array trap, which is composed of two capacitively coupled normal traps as shown in figure 1(b). In particular, they studied the charge transport in this system by using computer simulation taking into account cotunnelling, based on the tunnelling rate obtained from the approximation proposed by Fonseca *et al* [8]. When an excess electron is placed on one of the islands in the left-hand-side array, it is energetically favourable if there is a hole on the adjacent island in the right-hand-side array. Thus, an electron and a hole tend to pair and move together along the single-electron dual-junction array. According to the results of Amakawa *et al* [10], the lifetime of the electron–hole pair ('exciton') is longer than that of the single electron when the coupling capacitance C_C is large. This means that the binding energy of the electron–hole pair ('exciton') is so large that a tunnelling event in the left-hand-side array simultaneously induces a tunnelling event in the left-hand-side array when a small driving voltage is applied to the system. If the coupling capacitance decreases, the lifetime becomes shorter. This is due to the decrease in the binding energy of the 'exciton'; then the two arrays become virtually independent. Thus, this system

0953-8984/00/214641+13$30.00

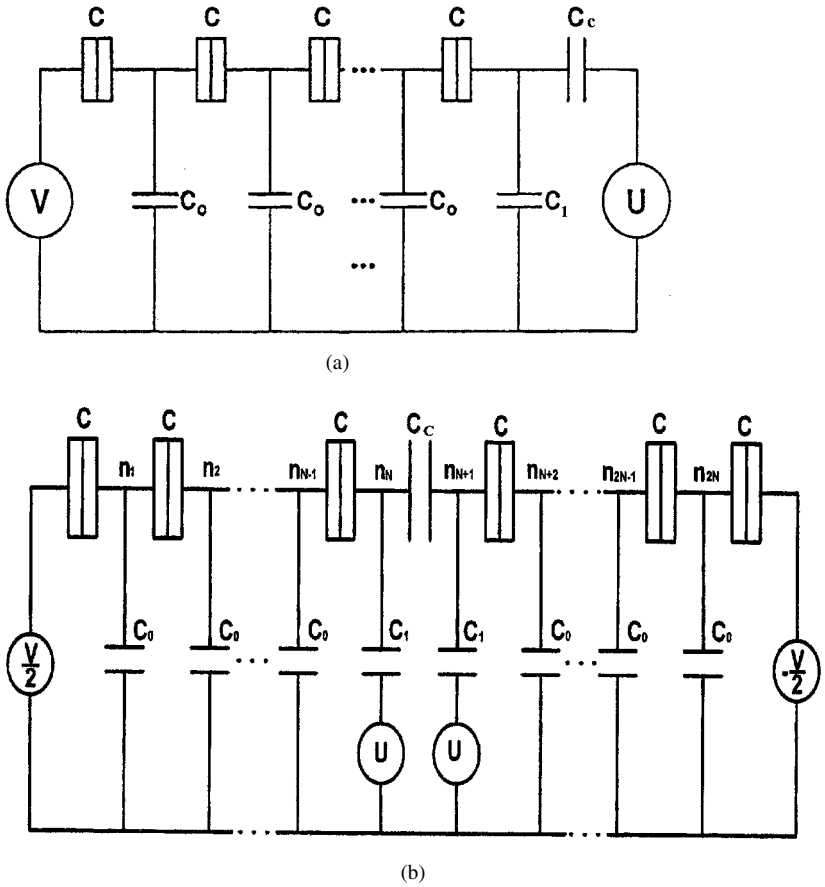

Figure 1. (a) The single-electron trap with N small junctions, with equal junction capacitances C, equal stray capacitances C_0, input gate capacitance C_1, and well capacitance C_C. The bias voltages of the two edges are V and U. (b) The single-electron dual-junction trap with $2N$ small junctions, with equal junction capacitances C, equal stray capacitances C_0, equal input gate capacitances C_1, and coupling capacitance C_C. The bias voltages of the two edges are $V/2$ and $-V/2$, while the voltages in the middle are U.

can also function as a memory cell by holding an electron–hole pair ('exciton') in the traps, i.e., a '0' state for no extra electron–hole pair ('exciton') in the traps and a '1' state for an electron–hole pair ('exciton') in the traps. In a sense, it could be considered as a single-'exciton' trap [2]. The remarkable thing here is that the earlier study was restricted to the case where the coupling capacitance is smaller than the junction capacitance and the role of the stray capacitance, which is known to be important in determining the soliton width in a one-dimensional (1D) array, was neglected.

The purpose of this study is to present an exact analytical solution to the electrostatic problem of the biased single-electron dual-junction-array trap consisting of equal stray capacitances C_0, equal junction capacitances C, equal input gate capacitances C_1, and coupling capacitance C_C, to derive analytical expressions for the total free energy and the threshold voltages for various charge-transfer processes (involving a single electron, a single exciton, and a combined soliton), and to study the effects of the stray capacitances, the input gate capacitances, the coupling capacitance, the number of junctions, and the cotunnelling process

on the threshold voltages of various charge solitons.

The starting point in studying the electrostatics of the single-electron dual-junction-array trap is to identify the potential profiles for a given set-up of the system. For a single-electron dual-junction-array trap with $2N$ junctions, one needs to solve a set of $2N$ linear equations for the corresponding voltages (or equivalently, the charges) on the $2N$ junctions. A set of $2N$ linear equations for the voltages $\{V_i\}$ across each of the $2N$ junctions are developed into a matrix form, and solved numerically without making any prior assumptions. The key to our approach is the rewriting of the electrostatic equations as matrix equations for the island potentials $\{\Phi_i\}$; this enables us to derive the electrostatic equations in a tridiagonal matrix form and obtain an exact analytic result for the single-electron dual-junction-array trap.

Although the bias voltage controls the average value of the current passing through the system, the dynamics of a single charge soliton in the system at $T = 0$ is in principle solely determined by the Gibbs free energy. The transfer of a soliton from one island to another through the tunnel junction between them is favourable if the Gibbs free energy decreases in this process, and vice versa. Thus, the essence of the dynamics is the evaluation of the Gibbs free energy, which consists of a charging energy term and a 'work done' term. The above-mentioned exact solutions of the electrostatics for the single-electron dual-junction-array trap enable us to perform systematic studies for the Gibbs free energy and derive an exact analytical form for it at arbitrary charge configurations. This allows us to predict many interesting behaviours of the system through the threshold voltage and compare them with numerical results reported previously by Amakawa *et al* [10].

The rest of the paper is organized as follows. In section 2, we obtain an exact analytic result for the island potentials $\{\Phi_i\}$ for the single-electron dual-junction-array trap, based on the study of the 1D array in reference [9]. With the island potentials obtained in section 2, an exact analytical form for the Gibbs free energy for arbitrary charge configurations will be derived in section 3. In section 4, we obtain the threshold voltages for various charge solitons including a single electron, a single exciton, and a combined soliton, using the exact analytical form for the Gibbs free energy. In section 5, we present the numerical results for the threshold voltages for various charge solitons, to investigate the effects of the stray capacitances, the input gate capacitances, the coupling capacitance, the number of junctions, and the cotunnelling process on the threshold voltages of various charge solitons. Conclusions will be given in the last section.

2. Potential profile

We consider a single-electron dual-junction-array trap, as illustrated in figure 1(b), where the ends of two single-electron traps are coupled to each other by a coupling capacitor C_C, and each single-electron trap consists of N small tunnel junctions in series, with equal stray capacitances C_0 and equal junction capacitances C, the end of which couples to an input gate capacitance C_1. The bias voltages of the two edges are $V/2$ and $-V/2$, while the voltages in the middle are U. Also, the tunnelling resistance R_T of each junction is assumed to be the same and $R_T \gg h/e^2$, which ensures that the wave function of an excess electron on an island is localized there. We denote the potential on each of the individual $2N$ islands between the junctions in the array by the column vector $\overline{\Phi} = \{\Phi_1, \Phi_2, \ldots, \Phi_{2N}\}^{\mathrm{T}}$, and the number of excess electrons on each of the individual $2N$ islands is denoted by the column vector $\overline{n} = \{n_1, n_2, \ldots, n_{2N}\}^{\mathrm{T}}$. The electrostatic equations for the island potentials $\{\Phi_i\}$ and the number of the excess island electrons $\{n_i\}$ are derived from the charge conservation and Kirchhoff's law, and they obey a set of $2N$ linear equations. These equations can be conveniently expressed in a simple form

as

$$\overline{\overline{S}}\,\overline{\Phi} = \frac{e}{C}\overline{n}' \tag{1}$$

where $\overline{n}'$ means that the first, the Nth, the $(N+1)$th, and the last elements of $\overline{n}'$ are replaced with $n_1 - CV/2e$, $n_N - C_1U/e$, $n_{N+1} - C_1U/e$, and $n_{2N} + CV/2e$, respectively, to accommodate the effects of the bias voltages and $\overline{\overline{S}}$ is a $2N$-by-$2N$ symmetric matrix given by

$$\overline{\overline{S}} = \begin{pmatrix} \overline{\overline{T}}_1 & \alpha\overline{\overline{1}} \\ \alpha\overline{\overline{1}}^{\mathrm{T}} & \overline{\overline{T}}_2 \end{pmatrix} \tag{2}$$

with

$$\overline{\overline{T}}_1 = \begin{pmatrix} \overline{\overline{M}} & \overline{1} \\ \overline{1}^{\mathrm{T}} & D' \end{pmatrix} \qquad \overline{\overline{T}}_2 = \begin{pmatrix} D' & \overline{1'}^{\mathrm{T}} \\ \overline{1}' & \overline{\overline{M}} \end{pmatrix} \tag{3}$$

$$\overline{\overline{1}} = \begin{pmatrix} \overline{0} & \overline{\overline{0}} \\ 1 & \overline{0}^{\mathrm{T}} \end{pmatrix} \qquad \overline{\overline{1}}^{\mathrm{T}} = \begin{pmatrix} \overline{0} & 1 \\ \overline{\overline{0}} & \overline{0} \end{pmatrix}. \tag{4}$$

Here, $\alpha = C_C/C$ is a coupling constant, $D' = -1-(C_1+C_C)/C$, $\overline{\overline{M}}$ is an $(N-1)$-by-$(N-1)$ symmetric tridiagonal matrix, having all diagonal elements the same, $D \equiv -(2+C_0/C)$, and all the off-diagonal elements equal to 1, and $\overline{\overline{0}}$ denotes an $(N-1)$-by-$(N-1)$ null matrix. In equations (3) and (4), the column vectors $\overline{1} = (0, 0, \ldots, 1)^{\mathrm{T}}$, $\overline{1}' = (1, 0, \ldots, 0)^{\mathrm{T}}$, and $\overline{0} = (0, 0, \ldots, 0)^{\mathrm{T}}$ each have $N-1$ elements.

Then, by using the matrix inverse to $\overline{\overline{S}}$, i.e., $\overline{\overline{H}}$, we obtain the analytical expression for the potential profiles in equation (1) as

$$\overline{\Phi} = \frac{e}{C}\overline{\overline{H}}\overline{n}' = \frac{e}{C}\begin{pmatrix} \overline{\overline{P}}_1 & \overline{\overline{Q}}_1 \\ \overline{\overline{Q}}_2 & \overline{\overline{P}}_2 \end{pmatrix}\overline{n}' \tag{5}$$

where the elements of the $2N$-by-$2N$ matrix $\overline{\overline{H}}$ have the following property: $H_{ij} = H_{ji} = H_{2N+1-j\,2N+1-i}$, and $\overline{\overline{P}}_1$, $\overline{\overline{P}}_2$, $\overline{\overline{Q}}_1$, and $\overline{\overline{Q}}_2$ are N-by-N symmetric sub-matrices of the matrix $\overline{\overline{H}}$. The symmetric matrix $\overline{\overline{P}}_1$ in equation (5) can be expressed by

$$\overline{\overline{P}}_1 = \begin{pmatrix} \overline{\overline{B}} & \dfrac{1}{D' + R_{N-1} - \alpha^2/(D' + R_{N-1})}\overline{R} \\ \dfrac{1}{D' + R_{N-1} - \alpha^2/(D' + R_{N-1})}\overline{R}^{\mathrm{T}} & \dfrac{1}{D' + R_{N-1} - \alpha^2/(D' + R_{N-1})} \end{pmatrix} \tag{6}$$

where the elements of the $(N-1)$-by-$(N-1)$ symmetric sub-matrix $\overline{\overline{B}}$ and the column vector $\overline{R}$ are, respectively, given by

$$(\overline{\overline{B}})_{ij} \equiv R'_{ij} = (-1)^{i+j+1} M'_{N-1-j} M_{N-1}/M'_{N-1} \qquad \text{for } i \leqslant j \text{ and } i, j \leqslant N-1 \tag{7}$$

$$R_i = \frac{\sinh\lambda}{\sinh N\lambda} \equiv R_{iN-1}. \tag{8}$$

Here,

$$M'_{j+1} = GM_j - M_{j-1}$$

with

$$M_j = (-1)^j \sinh(j+1)\lambda/\sinh\lambda \qquad G = D - 1/(D' - \alpha^2/(D' + R_{N-1})).$$

Also, λ is determined by $-2\cosh\lambda = D \equiv -(2 + C_0/C)$, and $R_{i,j}$ are the elements of the inverse matrix of an $(N-1)$-by-$(N-1)$ symmetric matrix $\overline{\overline{M}}$ in equation (3), which are given by

$$R_{ij} = -\frac{\cosh(N + |j-i|)\lambda - \cosh(N-j-i)\lambda}{2\sinh\lambda\sinh N\lambda} \qquad i, j = 1, 2, \ldots, N-1. \tag{9}$$

In addition, the elements of the N-by-N symmetric sub-matrices $\overline{\overline{P}}_2$, $\overline{\overline{Q}}_1$, and $\overline{\overline{Q}}_2$ in equation (5) are, respectively, given by

$$(\overline{\overline{P}}_2)_{ij} \equiv R'_{N+1-jN+1-i} = R'_{N+1-iN+1-j} \tag{10}$$

$$(\overline{\overline{Q}}_1)_{ij} = -\alpha R'_{N+1-jN} R_{iN} \tag{11}$$

$$(\overline{\overline{Q}}_2)_{ij} = -\alpha R_{NN+1-i} R'_{jN}. \tag{12}$$

It is to be noted that equation (5), supplemented by equations (6) and (10)–(12), is a general expression for the potential profile of the single-electron dual-junction-array trap with $2N$ tunnelling junctions with equal stray capacitances. If the value of α is taken as 0, equation (6) becomes identical to the expression for a symmetric matrix appearing in the potential profile for a normal trap obtained by Hu *et al* [9]. Moreover, equation (5) reduces to the Hu *et al* result [9] for the potential profile for a one-dimensional array with $2N+1$ tunnelling junctions with equal stray capacitances if the value of α is taken as 1. Equation (5), together with equations (6) and (10)–(12), is a basic result of this paper. Once a charge profile $\{n_i\}$ is known, we can use equation (5) to determine the potential profile $\{\Phi_i\}$ for the single-electron dual-junction-array trap.

3. Free energy and charging energy

In this section, we want to evaluate the Gibbs free energy of the single-electron dual-junction-array trap, by using the exact solution $\overline{\Phi}$ of equation (5). Since the free energy is a crucial quantity in determining the rate of tunnelling in small junctions, one needs to define it in a precise way. Basically, the free energy contains two terms, the electrostatic energy and the work done by moving the charged soliton through the system.

For a biased single-electron dual-junction-array trap as illustrated by figure 1(b), the Gibbs free energy can be written as

$$F = E_s + W \tag{13}$$

where the electrostatic energy is defined as

$$E_s = E_c - e\sum_{i=0}^{2N+1} n_i\Phi_i \tag{14}$$

with the charging energy

$$\begin{aligned} E_c = {} & \frac{C}{2}\sum_{i=1}^{N-1}(\Phi_{i+1}-\Phi_i)^2 + \frac{C}{2}\sum_{i=N+1}^{2N-1}(\Phi_{i+1}-\Phi_i)^2 + \frac{C}{2}\left(\Phi_1 - \frac{V}{2}\right)^2 \\ & + \frac{C}{2}\left(\Phi_{2N} + \frac{V}{2}\right)^2 + \frac{C_C}{2}(\Phi_{N+1}-\Phi_N)^2 + \frac{C_0}{2}\sum_{i=1}^{N-1}\Phi_i^2 + \frac{C_0}{2}\sum_{i=N+2}^{2N}\Phi_i^2 \\ & + \frac{C_1}{2}(U-\Phi_N)^2 + \frac{C_1}{2}(U-\Phi_{N+1})^2. \end{aligned} \tag{15}$$

In addition, in equation (13), the work due to the charge redistribution associated with the change of the charge profile $\{\overline{n}\}$ is given by

$$W = -C\sum_{i=1}^{N-1}(\Phi_{i+1}-\Phi_i)^2 - C\sum_{i=N+1}^{2N-1}(\Phi_{i+1}-\Phi_i)^2 - C_C(\Phi_{N+1}-\Phi_N)^2 - C\left(\Phi_1-\frac{V}{2}\right)^2 - C\left(\Phi_{2N}+\frac{V}{2}\right)^2 - C_0\sum_{i=1}^{N-1}\Phi_i^2 - C_0\sum_{i=N+2}^{2N}\Phi_i^2 - C_1(U-\Phi_N)^2 - C_1(U-\Phi_{N+1})^2. \tag{16}$$

In order to study the change of the Gibbs free energy in the event of a charge soliton transfer, it is desirable to rewrite it as a function of the charge profile $\{n_i\}$. For this purpose, after some algebra with equations (5) and (13)–(16), we can obtain the Gibbs free energy as

$$F = E_{ch} - \frac{e^2}{2C}\sum_{i=1}^{2N}\sum_{j=1}^{2N} n_i H_{ij} n_j - \frac{1}{2}V(Q_0 - Q_{2N+1}) - U(Q_N^g + Q_{N+1}^g) \tag{17}$$

where

$$E_{ch} = \frac{1}{4}CV^2(1 + H_{11} - H_{12N}) + C_1U^2\left(1 + \frac{C_1}{C}H_{NN} + \frac{C_1}{C}H_{NN+1}\right) \tag{18}$$

$$Q_N^g = C_1(U-\Phi_N) \qquad Q_{N+1}^g = C_1(U-\Phi_{N+1}) \tag{19}$$

$$Q_0 = n_0 e + C\left(\frac{V}{2} - \Phi_1\right) \qquad Q_{2N+1} = n_{2N+1}e + C\left(-\frac{V}{2} - \Phi_{2N}\right). \tag{20}$$

Equation (17) is a general expression for the Gibbs free energy of a single-electron dual-junction-array trap with bias voltage $\{V, U\}$, charge profile $\{n_i e\}$, and potential profile $\{\Phi_i\}$ on the islands. On the basis of the Gibbs free energy (17), one can directly study the dynamics of the single-electron tunnelling by calculating the change of the Gibbs free energy ΔF due to some charge-transfer event. To be definite, here we discuss the case where the charge transfer happened between two islands k and k', while the charges on the other islands are unchanged. We assume, however, that the tunnelling between two islands N and $N+1$ is negligible, so that we have two circuits that are independent galvanically but are coupled electrostatically [2]. We denote the charges on these islands before and after the charge transfer as $\{n_k, n_{k'}\}$ and $\{n'_k, n'_{k'}\}$, respectively, and the net transferred charges as Q, where Q can be a single electron, a single exciton, or a combined soliton, which will be discussed in the next section. Thus, we obtain, from equation (17), the change of the Gibbs free energy $\Delta F^Q(k,k')$ due to the charge transfer $\{n_k, n_{k'}\}$ to $\{n'_k, n'_{k'}\}$:

$$\Delta F^Q(k,k') \equiv F(\{n'_k, n'_{k'}\}) - F(\{n_k, n_{k'}\}) = \Delta E^Q(k,k') + W^Q(k,k') \tag{21}$$

where the detailed form of the change of the charging energy $\Delta E^Q(k,k')$ and the work done $W^Q(k,k')$ in equation (21) can be directly worked out from equation (17).

4. Threshold voltage

Now, let us calculate the change of the Gibbs free energy $\Delta F^Q(k,k')$ due to some charge transfer by means of equation (21). Here we consider three cases of particular interest:

(i) the *single-charge-soliton (e)* case, where an electron is transferred from the kth island to the k'th island in the left-hand-side array, i.e., $n'_k - n_k = -1$, $n'_{k'} - n_{k'} = 1$, $n'_{2N-k+1} - n_{2N-k+1} = 0$, $n'_{2N-k'+1} - n_{2N-k'+1} = 0$;

(ii) the *exciton soliton (electron–hole pair, ex) case*, where an electron in the left-hand-side array is transferred from the kth island to the k'th island and an electron in the right-hand-side array is simultaneously transferred from the $(2N - k' + 1)$th island to the $(2N - k + 1)$th island, i.e., $n'_k - n_k = -1$, $n'_{k'} - n_{k'} = 1$, $n'_{2N-k+1} - n_{2N-k+1} = 1$, $n'_{2N-k'+1} - n_{2N-k'+1} = -1$;

(iii) the *combined soliton (exciton–single electron, ex–e) case*, where in addition to the exciton case, an electron in the left-hand-side array is transferred from the k'th island to the k''th island, i.e., $n'_k - n_k = -1$, $n'_{k'} - n_{k'} = 0$, $n'_{k''} - n_{k''} = 1$, $n'_{2N-k+1} - n_{2N-k+1} = 1$, $n'_{2N-k'+1} - n_{2N-k'+1} = -1$.

Under the above conditions, the change of the Gibbs free energy for each *charge soliton transfer* can be derived from equation (17) as

$$\begin{aligned}\Delta F^e(k,k') &= F^e(k') - F^e(k)\\ &= -\frac{e^2}{2C}(H_{k'k'} - H_{kk})\\ &\quad -\frac{1}{2}eV(\delta_{0,k'} - \delta_{0,k} - \delta_{2N+1,k'} + \delta_{2N+1,k} - H_{1k'} + H_{2Nk'} + H_{1k} - H_{2Nk}) \qquad (22)\end{aligned}$$

$$\begin{aligned}\Delta F^{ex}(k,k') &= F^{ex}(k') - F^{ex}(k)\\ &= -\frac{e^2}{C}(H_{k'k'} - H_{k'2N-k'+1} - H_{kk} + H_{k2N-k+1})\\ &\quad -\frac{1}{2}eV(\delta_{0,k'} + \delta_{2N+1,2N-k'+1} - \delta_{0,k} - \delta_{2N+1,2N-k+1})\\ &\quad + eV(H_{1k'} - H_{12N-k'+1} - H_{1k} + H_{12N-k+1}) \qquad (23)\end{aligned}$$

$$\begin{aligned}\Delta F^{ex-e}(k,k';k'') &= F^{ex-e}(k',k'') - F^{ex-e}(k)\\ &= -\frac{e^2}{2C}(H_{k''k''} + H_{k'k'} - 2H_{k''2N-k'+1} - H_{kk} + H_{k2N-k+1})\\ &\quad -\frac{1}{2}eV(\delta_{0,k''} + \delta_{2N+1,2N-k'+1} - \delta_{0,k} - \delta_{2N+1,2N-k+1})\\ &\quad +\frac{1}{2}eV(H_{1k''} - H_{12N-k'+1} - H_{12N-k''+1} + H_{1k'} - 2H_{1k} + 2H_{12N-k+1}) \qquad (24)\end{aligned}$$

where the bias voltage U was taken as 0 for convenience.

The tunnelling of a charge soliton from the kth island to the k'th island in the single-electron dual-junction-array trap is energetically favourable when the free energy $\Delta F^Q(k,k')$ is less than zero, and vice versa. Thus, the threshold energy V_t for the transfer of a charge soliton from the kth island onto the k'th island can be obtained by equating $\Delta F^Q(k,k')$ to zero. Applying this principle to equations (22)–(24), we can obtain the threshold voltages for various *charge-soliton-transfer* cases as

$$\begin{aligned}V_t^e(k,k') &= \frac{e}{C}(H_{k'k'} - H_{kk})\\ &\quad \times [\delta_{0,k'} - \delta_{0,k} - \delta_{2N+1,k'} + \delta_{2N+1,k} - H_{1k'} + H_{2Nk'} + H_{1k} - H_{2Nk}]^{-1} \qquad (25)\end{aligned}$$

$$\begin{aligned}V_t^{ex}(k,k') &= \frac{2e}{C}(H_{k'k'} - H_{k'2N-k'+1} - H_{kk} + H_{k2N-k+1})\\ &\quad \times [(\delta_{0,k} + \delta_{2N+1,2N-k+1} - \delta_{0,k'} - \delta_{2N+1,2N-k'+1})\\ &\quad + 2(H_{1k'} - H_{12N-k'+1} - H_{1k} + H_{12N-k+1})]^{-1} \qquad (26)\end{aligned}$$

$$V_t^{ex-e}(k;k',k'') = \frac{2e}{C}(H_{k'k'} - H_{k'2N-k'+1} - H_{kk} + H_{k2N-k+1}) \times[(-\delta_{0,k'} - \delta_{2N+1,2N-k'+1} + \delta_{0,k} + \delta_{2N+1,2N-k+1}) + 2(H_{12N-k'+1} - H_{1k'} - H_{12N-k+1} + H_{1k})]^{-1}. \quad (27)$$

Equations (25)–(27) are key results giving the threshold voltages for various *charge-soliton-transfer* cases, which enable us to analyse the charge transport in the single-electron dual-junction-array trap. It is clearly seen from equations (25)–(27) that the threshold voltages are very sensitive to the cotunnelling process, the number of junctions N, the coupling capacitance C_C, the stray capacitance C_0, and the junction capacitance C, as well as the input gate capacitance C_1 through the elements of the $2N$-by-$2N$ symmetric matrix $\overline{\overline{H}}$.

5. Numerical results

In this section, we present the numerical results for the threshold voltages obtained for various charge-soliton-transfer processes (involving a single electron, an exciton, and a combined soliton). First, we study the dependence on C_0, C_1, C_C, and C of the threshold voltages for various charge-soliton-transfer processes in the case where one-junction tunnelling, i.e., m ($\equiv k' - k$) $= 1$ for $k = 0$ in equations (25)–(27), is allowed in the single-electron dual-junction-array trap having only three tunnel junctions ($N = 3$) on each array side, and then perform an analysis of the dependences on N and the cotunnelling of the threshold voltages at fixed values of C_1, C_C, and C for various stray capacitances, as an example.

The stray capacitance dependence of the threshold voltages (in units of e/C) is illustrated for various charge solitons in figure 2, where we plot the threshold voltages in equations (25)–(27) as functions of the ratio of stay capacitance to junction capacitance, i.e., $\eta = C_0/C$, at $\beta = C_1/C = 0.05, 1, 10$ and $\alpha = C_C/C = 0.5$. It is clearly seen from the figure that the threshold voltages of all charge solitons decrease with the increase of the value of η. For $\eta \to 0$ and small β (<1), the exciton has a lower threshold voltage than any other soliton. This means that the exciton transport is dominant in the system, as reported by Amakawa *et al* [10]. However, as can be seen from the inset, which shows an enlarged view of the small-η region, for large β ($\geqslant 1$) the combined soliton has the lowest threshold voltage and is expected to be dominant. Thus, for no stray capacitance, the solitons which are dominant in the system are either single excitons or combined solitons depending on the input gate capacitance. The small change of η in the small-η (<1) region leads to a lot of change in the threshold voltage, but the threshold voltages are almost constant in the large-η (>1) region. The interesting feature is the $\beta = 1$ case. For small η ($\leqslant 1$), the combined soliton has the lowest threshold voltage, while for large η (>1), the single electron or exciton has the lowest threshold voltage. Thus, the dominant soliton transport varies with the stray capacitance. Moreover, the threshold voltage of the exciton merges into that of the single electron for small η and large β or large η and small β. In that case, single-electron and exciton transport coexist and will be dominant. For large β and η, however, the combined soliton transport is expected to be dominant.

Figure 3 shows the dependence of the threshold voltage (in units of e/C) on the input gate capacitance for various charge solitons, where we plot the threshold voltages in equations (25)–(27) as functions of the ratio of input gate capacitance to junction capacitance, i.e., $\beta = C_1/C$, at $\alpha = 0.5$ for various stray capacitances of $\eta = 0.5, 1, 5$. As can be seen from the figure, if the value of β increases for a specific value of η, the threshold voltages of the single electron and exciton remain constant, whereas those of the combined soliton decrease. As a result, a change in the type of soliton transport is expected with the increase of β. For small η, exciton transport dominates in the small-β region, but if the value of β increases, the combined soliton

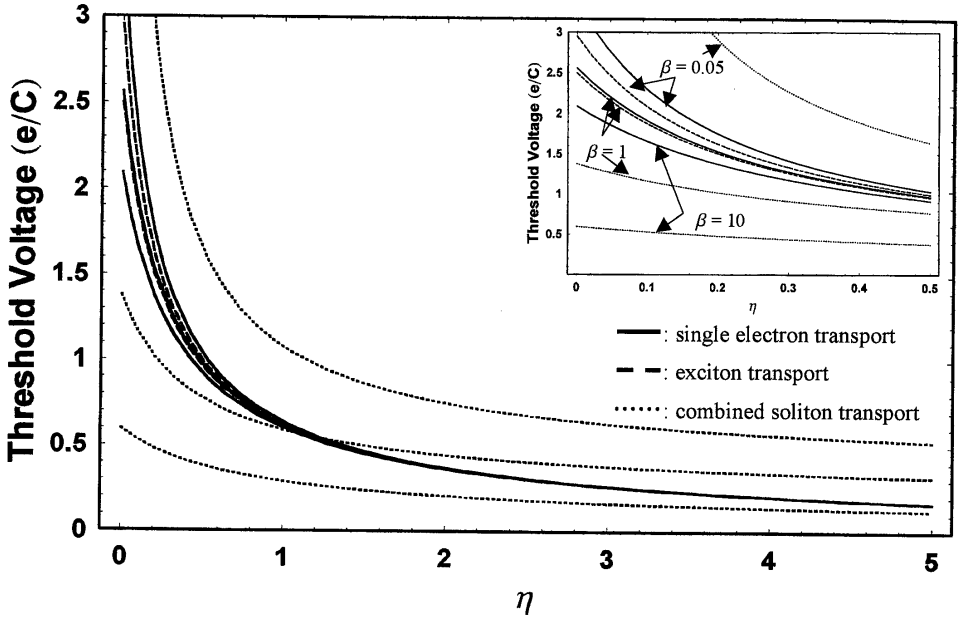

Figure 2. Threshold voltages (in units of e/C) for injecting a charge soliton into the first island of a single-electron dual-junction-array trap with three junctions ($N = 3$) on each side as functions of $\eta = C_0/C$ at $\beta = C_1/C = 0.05, 1, 10$ and $\alpha = C_C/C = 0.5$. Shown in the inset is an enlarged view of the small-α region. Also, C_C, C_1, C, and C_0 are the coupling capacitance, input gate capacitance, junction capacitance, and stray capacitance, respectively.

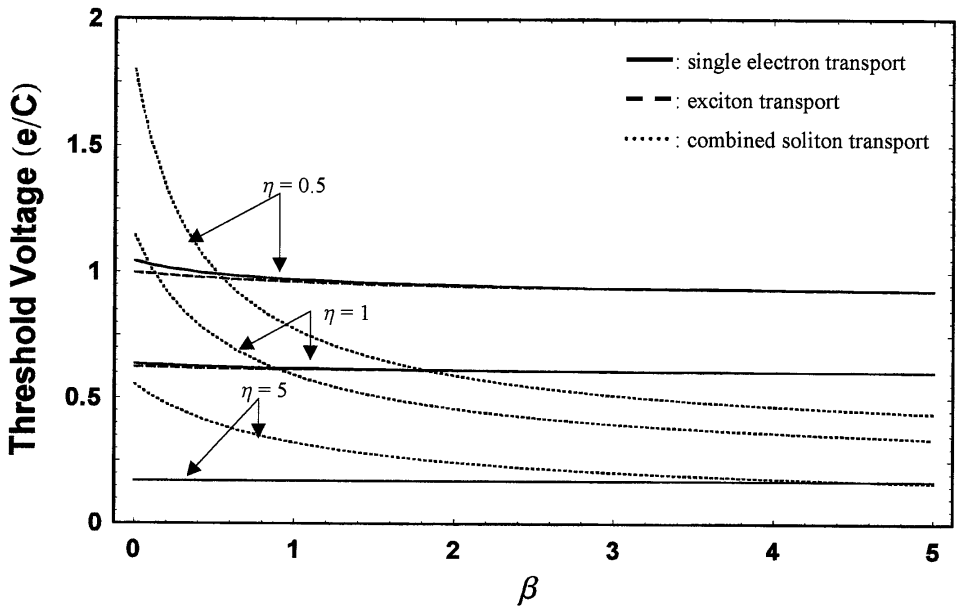

Figure 3. Threshold voltages (in units of e/C) for injecting a charge soliton into the first island of a single-electron dual-junction-array trap with three junctions ($N = 3$) on each side as functions of $\beta = C_1/C$ at $\alpha = C_C/C = 0.5$ and $\eta = C_0/C = 0.5, 1, 5$, where C_C, C_1, C, and C_0 are the coupling capacitance, input gate capacitance, junction capacitance, and stray capacitance, respectively.

becomes dominant. Furthermore, if the values of β and η increase, the slight difference in threshold voltage between the exciton and single electron disappears. Then, both types of soliton transport will be dominant for large η and small β. Thus, the charge soliton transport is sensitive to the values of the stray capacitance C_0, the junction capacitance C, and the input gate capacitance C_1. The results shown in figures 2 and 3 are restricted to the specific value of $\alpha = 0.5$.

The threshold voltages (in units of e/C) for various charge solitons are shown in figure 4, as functions of the ratio of coupling capacitance to junction capacitance, i.e., $\alpha = C_C/C$, at $\eta = 0.05$ for various input gate capacitances of $\beta = 0.5, 1, 5$. This figure shows that the threshold voltages of all charge solitons remain constant, except for small α and β. If the coupling capacitance approaches zero, or the value of β increases, the threshold voltage of the exciton merges into that of the single electron. However, their threshold voltages have larger values than that of the combined soliton. As shown in the figure, for given parameters β and η the combined soliton has a lower threshold voltage than any other soliton and hence combined soliton transport is expected to be dominant for all given α. It should be noted that the results given in figures 1, 2, and 3 are valid for $N = 3$ and one-junction tunnelling. As discussed before, the threshold voltages of charge solitons are influenced by the parameters characterizing the system, such as the coupling capacitance C_C, the stray capacitance C_0, and the junction capacitance C, as well as the input gate capacitance C_1. In addition, the cotunnelling effect and the number of junctions N also affect the threshold voltages of charge solitons.

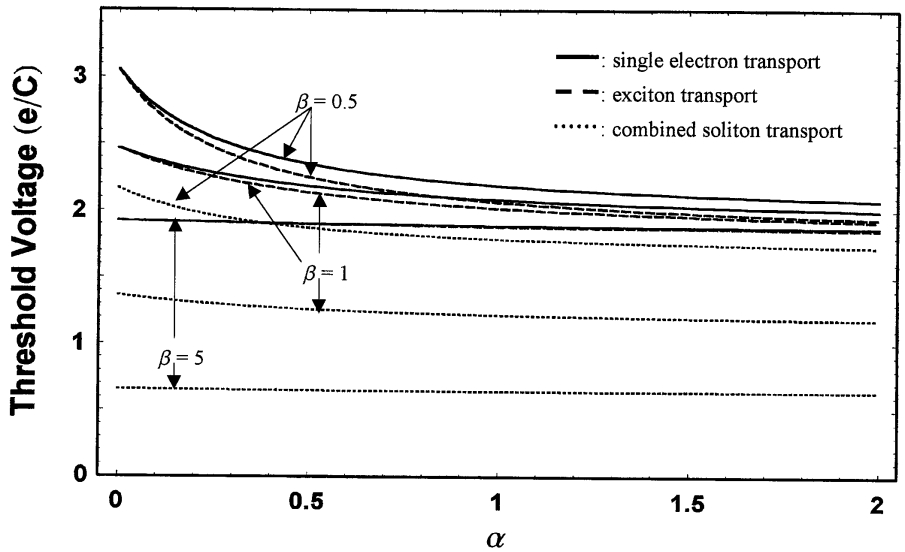

Figure 4. Threshold voltages (in units of e/C) for injecting a charge soliton into the first island of a single-electron dual-junction-array trap with three junctions ($N = 3$) on each side as functions of $\alpha = C_C/C$ at $\eta = C_0/C = 0.05$ and $\beta = C_1/C = 0.5, 1, 5$, where C_C, C_1, C, and C_0 are the coupling capacitance, input gate capacitance, junction capacitance, and stray capacitance, respectively.

Figure 5 shows the dependences of the threshold voltages for various charge solitons on the number of junctions N at a fixed value of $\alpha = \beta = 0.5$ for various stray capacitances $\eta = 0.05, 1, 5$. It is clearly seen from the figure that, as mentioned with reference to figure 2, the threshold voltage decreases with the increase of the stray capacitance and change of which soliton is dominant in the transport is expected for $N \leqslant 3$, rather than $N > 3$. Comparing

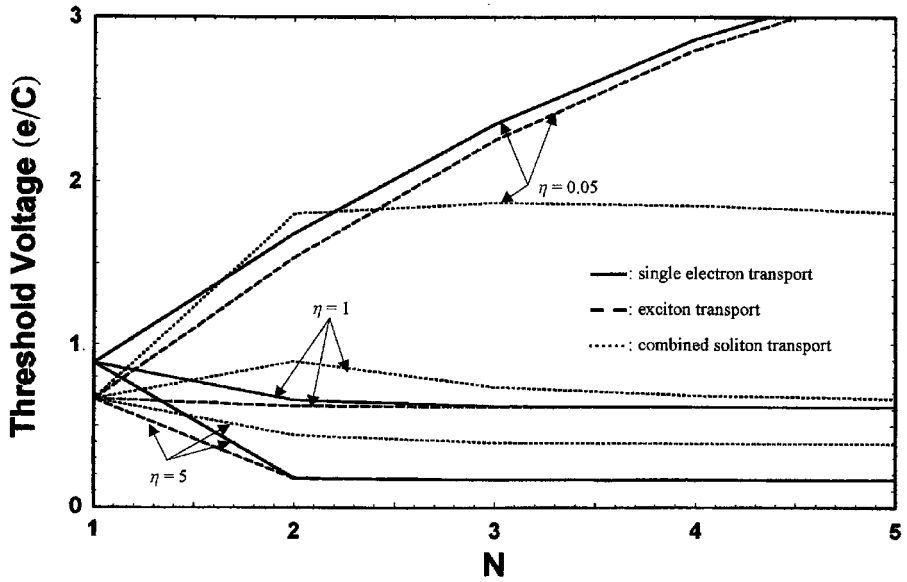

Figure 5. Threshold voltages for injecting a charge soliton into the first island of a single-electron dual-junction-array trap as functions of the number of junctions N at a fixed value of $\alpha = C_C/C = \beta = C_1/C = 0.5$ and $\eta = C_0/C = 0.05, 1, 5$, where C_C, C_1, C, and C_0 are the coupling capacitance, input gate capacitance, junction capacitance, and stray capacitance, respectively.

the threshold voltages of charge solitons for $N = 2$ and those of charge solitons for $N = 3$ in the case of small η, we can see that the exciton transport is expected to be dominant for $N = 2$, whereas the combined soliton transport is dominant for $N = 3$. Thus, change in the number of junctions can lead to a change in the type of charge soliton transport. This is valid for $\alpha = \beta = 0.5$. Note that the N-dependence of the threshold voltages for various charge solitons varies with the values of α and β, as is expected from figures 2, 3, and 4.

The dependence on cotunnelling (m) of the threshold voltages is shown in figure 6 for various charge solitons, where the circuit parameters were taken as $N = 10$, $\alpha = \beta = 0.5$, and $\eta = 0.5, 1, 5$ as an example. As shown in the figure, the threshold voltages have various dependences on the cotunnelling according to the stray capacitance. For small η ($\leqslant 1$), change of which soliton is dominant in the transport, from the combined soliton to the exciton, is expected as the cotunnelling is increased. However, one can see that if the stray capacitance increases, single-electron or exciton transport becomes dominant because the threshold voltages for the single electron and the exciton are nearly same. Thus, we can see that the threshold voltages of solitons can be influenced by the effect of cotunnelling. The results are restricted to the special cases of $N = 10$, $\alpha = \beta = 0.5$, and $\eta = 0.5, 1, 5$. It should be noted that, as can be expected from previous figures, the threshold voltages of charge solitons can show different cotunnelling dependences, according to the values of N, α, β, and η.

6. Conclusions

So far, we have presented an exact solution for the potential profiles of the biased single-electron dual-junction-array trap with equal stray capacitances. On the basis of equation (5), we have

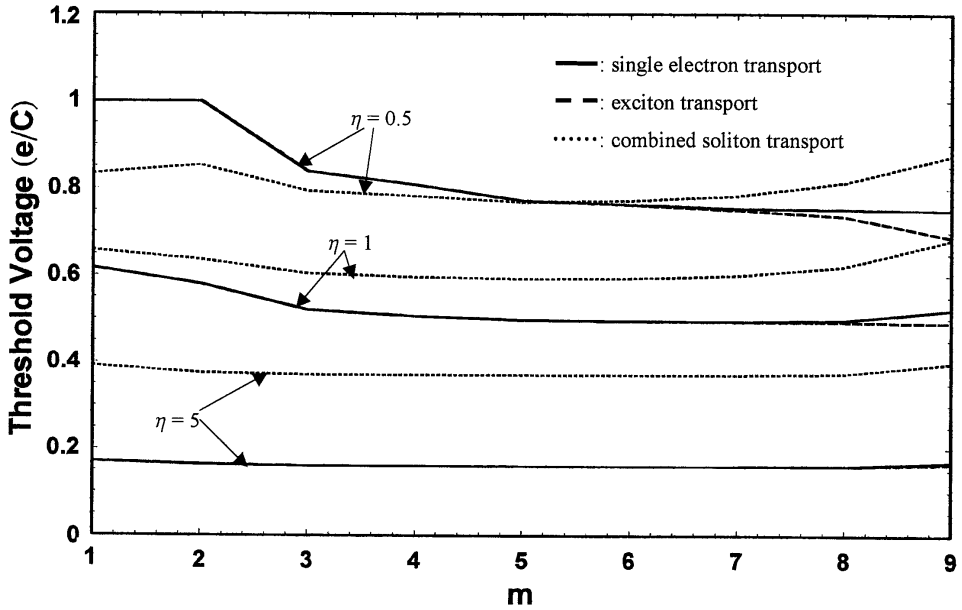

Figure 6. Threshold voltages of a single-electron dual-junction-array trap with ten junctions ($N = 10$) on each side as functions of the cotunnelling (m) at $\alpha = C_C/C = \beta = C_1/C = 0.5$, and $\eta = C_0/C = 0.5, 1, 5$, where C_C, C_1, C, and C_0 are the coupling capacitance, input gate capacitance, junction capacitance, and stray capacitance, respectively.

obtained an analytical Gibbs free energy, as well as the threshold voltages of equations (25)–(27), for various charge solitons including a single electron, an exciton, and a combined soliton. With the threshold voltage obtained, we have performed a numerical analysis, in order to understand the dependence of threshold voltages on the stray capacitance, the coupling capacitance, the input gate capacitance, and the number of junctions, as well as the cotunnelling.

Our results for the case where one-junction tunnelling is allowed in the single-electron dual-junction-array trap having only three tunnel junctions ($N = 3$) on each side show that the threshold voltages of all charge solitons decrease with the increase of the stray capacitance. For no stray capacitance and weak coupling and input gate capacitances, the exciton transport becomes dominant in the system, as reported by Amakawa *et al* [10]. However, if the input gate capacitance is increased, the combined charge soliton has a lower threshold voltage than any other charge soliton and it becomes dominant in transport. Thus, for no stray capacitance, the solitons which are dominant in the system can be single excitons or combined solitons according to the input gate capacitance. A lot of change in threshold voltage in the small-stray-capacitance region is expected, but the threshold voltages are almost constant in the large-stray-capacitance region. In consequence, for the case where the input gate capacitance is the same as the junction capacitance, the dominant soliton in transport can be a combined soliton, a single electron, or an exciton, depending on the stray capacitance. Thus, for a specific coupling capacitance, the dominant soliton in transport can be a combined soliton, a single electron, or an exciton, according to the stray capacitance and the input gate capacitance.

Various charge solitons having the lowest threshold voltages are also expected for specific values of the coupling capacitance, the input gate capacitance, and the stray capacitance as the number of junctions changes. In particular, change of which soliton is dominant in the transport is expected for $N \leqslant 3$, rather than $N > 3$, for the special values $\alpha = \beta = 0.5$.

Comparing the threshold voltages of charge solitons for $N = 2$ and those of charge solitons for $N = 3$ in the case of small η, we can see that the exciton transport is expected to be dominant for $N = 2$, whereas the combined soliton transport is dominant for $N = 3$. Thus, the change of the number of junctions leads to a change in the type of charge soliton transport. In addition, the effect of cotunnelling, which is sensitive to the stray capacitance, plays an important role in determining which solitons are dominant in the system. For small stray capacitance, change of which soliton is dominant in the transport from the combined soliton to the exciton is expected as the cotunnelling is increased. However, one can see that if the stray capacitance increases, the single-electron or exciton transport becomes dominant because the threshold voltages for the single electron and exciton are nearly same. Thus, various types of charge soliton transport are expected, depending on the parameters characterizing the system, such as the coupling capacitance C_C, the stray capacitance C_0, the junction capacitance C, the input gate capacitance C_1, and the number of junctions, as well as the cotunnelling.

We conclude that, in studying the charge transport of the biased single-electron dual-junction-array trap with equal stray capacitances, it is necessary to treat the electrostatic problem exactly. The quantitative behaviour identified in this paper should provide useful information pertaining to future experiments.

Acknowledgments

This work was supported in part by the LG Foundation, Korea, and in part by the Texas Center for Superconductivity at the University of Houston, USA.

References

[1] Likharev K K 1988 *IBM J. Res. Dev.* **32** 144
[2] Averin D V, Korotkov A N and Nazarov Yu V 1991 *Phys. Rev. Lett.* **66** 2818
[3] Grabert H and Devoret M H (ed) 1992 *Single Charge Tunneling (NATO ASI Series B)* (New York: Plenum) ch 7, p 249 and references therein
[4] Averin D V, Odintsov A A and Vyshenskii S V 1993 *J. Appl. Phys.* **73** 1297
[5] Bauernschmitt R and Nazarov Y V 1993 *Phys. Rev.* B **47** 9997
[6] Nakazato K, Blaikie R J and Ahmed H 1994 *J. Appl. Phys.* **75** 5123
[7] Dresselhaus P D, Ji L, Han S, Lukens J E and Likharev K K 1994 *Phys. Rev. Lett.* **72** 3226
[8] Fonseca L R C, Korotkov A N, Likharev K K and Odintsov A A 1995 *J. Appl. Phys.* **78** 3238
[9] Hu G Y, O'Connell R F, Kang Y B and Ryu J Y 1996 *Int. J. Mod. Phys.* B **10** 2441
[10] Amakawa S, Fujishima M and Hoh K 1996 Dual-junction-array single electron trap *The Electrochemical Society October Meeting* vol 2 (Princeton, NJ: The Electrochemical Society) p 572
[11] Matters M, Versluys J J and Mooij J E 1997 *Phys. Rev. Lett.* **78** 2469
[12] Matsuoka K A, Likharev K K, Dresselhaus P, Ji L, Han S and Lukens J 1997 *J. Appl. Phys.* **81** 2269